Ice stream D flow speed is strongly modulated by the tide beneath the Ross Ice Shelf

S. Anandakrishnan, D. E. Voigt, and R. B. Alley

Earth and Mineral Sciences Environment Institute, Department of Geosciences, Pennsylvania State University, University Park, Pennsylvania, USA

M. A. King

School of Civil Engineering and Geosciences, University of Newcastle Upon Tyne, Newcastle Upon Tyne, UK

Received 24 September 2002; revised 12 November 2002; accepted 21 January 2003; published 2 April 2003.

[1] The flow velocity of ice stream D, West Antarctica has been measured to vary by a factor of three over the course of a day. These fluctuations are measured at the grounding line as well as upstream of the grounding line in the ice plain of ice stream D. The diurnal velocity fluctations appear to be driven by the tide beneath the Ross Ice Shelf. These results suggest that there is significant, and heretofore poorly understood, influence of the ocean tide and of the ice shelf on the dynamics of ice stream flow. *INDEX TERMS:* 1827 Hydrology: Glaciology (1863); 1863 Hydrology: Snow and ice (1827); 1255 Geodesy and Gravity: Tides—ocean (4560). **Citation:** Anandakrishnan, S., D. E. Voigt, R. B. Alley, and M. A. King, Ice stream D flow speed is strongly modulated by the tide beneath the Ross Ice Shelf, *Geophys. Res. Lett.*, *30*(7), 1361, doi:10.1029/2002GL016329, 2003.

1. Introduction and Data Collection

[2] Most ice streams and outlet glaciers in Antarctica discharge either into extensive ice shelves or directly into the open ocean. As a result, the ice at the grounding lines is acted upon by the forces of the ocean tide, which affect both the open ocean and the ice-shelf-covered seas. These forces have been measured to affect the ice shelves themselves and the region of the ice streams within a few kilometers of their grounding lines [*Williams and Robinson*, 1980; *Doake et al.*, 2002; *Smith*, 1991; *Doake et al.*, 1987; *Goldstein et al.*, 1993]. In one case the rate of basal seismicity of ice stream C, a nearly quiescent glacier, has been shown to vary with the tide [*Anandakrishnan and Alley*, 1997]. In another case the earth tide modulated the basal water system of an alpine glacier [*Kulessa et al.*, 2003].

[3] Aside from these selected examples, theories of ice-stream, ice-shelf, and outlet glacier dynamics do not generally consider the influence of ocean tides or the earth tide as factors influencing flow. In the past, the ability to detect small flow variations on a diurnal time scale was poor. The results of this study (and those of *Bindschadler et al.* [2003] for ice stream B) provide a first-ever view of the flow of a major ice stream where tidal-frequency fluctuations are resolved. We suggest that theories and models for flow in the ice plains of ice streams (and perhaps farther inland where there is evidence of diurnal fluctuations in water pressure [*Harrison et al.*, 1993; *Engelhardt and Kamb*, 1998], strain rate, and seismicity [*Harrison et al.*, 1993]) will need to take into account tidal forcings.

[4] The flow velocity of ice stream D, West Antarctica was measured at 3 locations, and a base station was established on slow-moving, non-ice-stream Siple Dome (SDM) using dual-frequency GPS (Global Positioning System) receivers (see Table 1 and Figure 1). The stations were sited at the grounding line (K0), 40 km upstream of K0 along the central flow line of ice stream D (K40), and 80 upstream of K0 (K80). K80 was not on the central flow line of ice stream D due to the presence of large crevasses there; K80 is closer to the northern shear margin of the ice stream. The stations were occupied for 24 days in November and December of 2000. The GPS antennae and ground planes were mounted on 2 m steel poles driven into the snow surface. The continuously operating GPS receivers logged data at 60 s intervals.

1.1. Data Collection and Analysis

[5] The GPS data were analyzed using kinematic Precise Point Positioning (PPP) algorithms [*Zumberge et al.*, 1997] to solve station coordinates at 5 minute intervals over the course of the experiment [*King and Aoki*, 2003]. It is important that kinematic algorithms were adopted since other approaches (e.g., static sub-daily solutions) will result in horizontal coordinate bias when measuring on a moving surface. Using PPP as implemented in the GIPSY [*Lichten*, 1990] software, we have been able to routinely obtain coordinate estimates every 5 minutes with repeatabilities of 30–40 mm, modelling the antenna motion as a random walk process. Such repeatabilities are possible because the motion of the ice is relatively slow, allowing for the filter process noise covariance [*Lichten*, 1990] to be reduced. By taking care that the filter is not over-constrained, very high precision coordinates may be obtained without filtering the time series significantly, and without introducing processing artifacts. The resulting coordinates were converted to a local geodetic coordinate system (easting and northing relative to the first position in the time series), and in our subsequent discussion of the "position of a station", we are referring to the relative position.

[6] The vertical positions at K0 (Figure 2, top curve; the abscissa is 10 days of the experiment that encompass the spring tide) show the rising and falling of the ice surface with the ocean tide beneath the Ross Ice Shelf. We use the vertical position at K0 as a proxy for the tidal forcing (see *MacAyeal* [1984] and *Padman et al.* [2002] for a review of the tides beneath the Ross Ice Shelf).

Copyright 2003 by the American Geophysical Union.
0094-8276/03/2002GL016329$05.00

Table 1. GPS Station Locations and Mean Velocities Calculated from the Full Data Set

Site	Latitude	Longitude	Speed(m · d^{-1})
K0	S80°23′59.5″	W150°00′01″	1.22
K40	S80°32′17.3″	W147°58′16″	1.21
K80	S80°40′45.2″	W145°37′28.5″	0.616
SDM1	S81°39′10.9″	W149°00′01.0″	0.

[7] The mean velocity of each of the stations is the slope of the inline position data (see Table 1), and each compares well to other measurements [*Joughin et al.*, 1999]. The detrended inline positions (the mean displacement is removed) of the three ice stream sites K0, K40, and K80 are plotted in the lower panel of Figure 2. These data illustrate the large variation in flow over the course of a day. The period of these fluctuations is the same as that of the tide beneath the Ross Ice Shelf (upper panel of Figure 2). The ordinates are the along-flow variations in position relative to the mean position that would have been occupied if the sites were moving at a constant velocity (for display we have offset the K0 and K80 data by +0.15 m and −0.15 m, respectively). These data show the dramatic variation in flow over the course of a day at all the stations, but most strikingly at the grounding line. The velocity is the derivative of these positions (added to the mean velocity), and it is apparent that the velocity peaks at all three sites during the falling tide and the velocity reaches a minimum during the rising tide. The magnitude of the velocity fluctuation is approximately $v_f \sim \pm 0.7\text{m} \cdot \text{d}^{-1}$, compared to a mean flow speed of $\bar{v} = 1.2$ m · d^{-1} at K0 and K40, and $\bar{v} = 0.62$ m · d^{-1} at K80. The amplitude of the flow fluctuations do not mirror the tidal range, suggesting that the transfer function between tidal range and flow fluctuations is non-linear. There also appear to be episodic movements (similar to those observed by *Bindschadler et al.* [in press], but not as large or as regular).

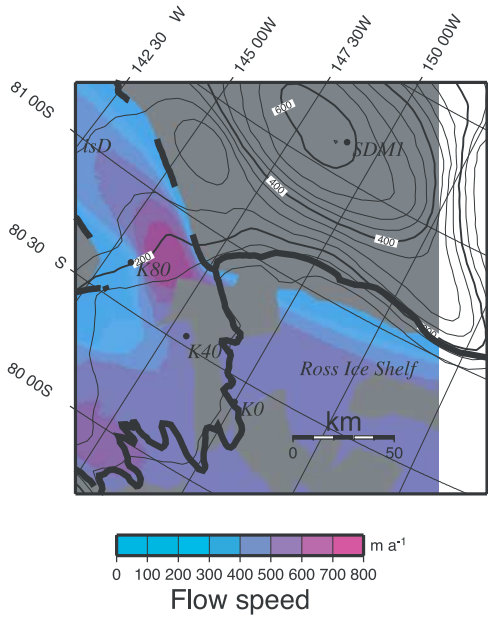

Figure 1. Map of the grounding line and ice plain region of ice stream D, E, and Siple Dome. The surface elevation contours are from the Radarsat Digital Elevation Model [*Liu et al.*, 2001]. The flow speeds are from *Joughin et al.* [1999]; note that in the text we use m · d^{-1}. To convert from m·a^{-1} and m · d^{-1}, divide these values by 365.25. The heavy black line is the grounding line of the ice streams, picked from Landsat imagery (P. Vornberger, personal communication, 2001). K0, K40, K80, and SDM1 are the locations of the four GPS stations discussed in the text.

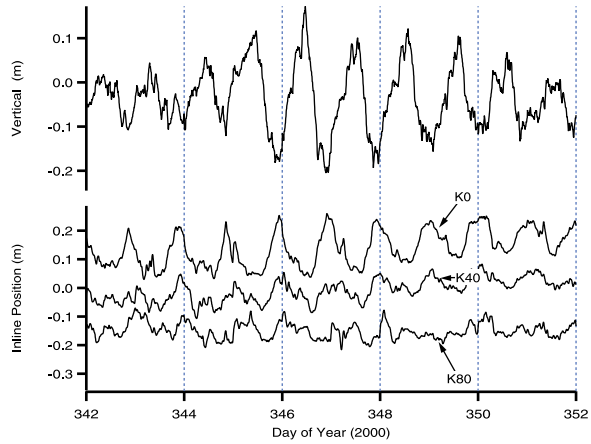

Figure 2. Vertical position at Site K0 (upper panel) and the detrended inline positions (lower panel) at the grounding line (K0-upper curve), at site K40 (center curve) and at site K80 (lower curve). The three curves all have zero mean but K0 and K80 have been offset for display purposes. The abscissa is 10 days of the year 2000.

2. Flow Discussion

2.1. Flow Field at K0

[8] At the grounding line (station K0), the ice stream speeds up during the falling tide and slows during the rising tide (Figure 3). There is a weak dependence between tide amplitude and velocity fluctuation v_f, but the main result is that the velocity fluctuates by ±0.7 m · d^{-1}, a range that is comparable to the mean flow speed of $\bar{v} = 1.2$ m · d^{-1}. Thus, at the grounding line ice stream D has a factor of three variation in flow speed over the course of a tidal cycle (which is approximately 24 hrs in the eastern Ross Ice Shelf [*Padman et al.*, 2002]). The cross-correlation of the inline velocity at K0 and the tidal signal shows that the velocity extrema lag the tidal extrema by 6 ± 1 hrs (i.e., high tide is followed six hours later by high velocity, and low tide is followed by low velocity).

[9] The crossline flow also shows a significant side-to-side behavior (Figure 4) that has not been previously observed. The ice flows to the south (left of the predominantly westwards flow of ice stream D) during the rising tide and to the north during the falling tide. The crossline displacement fluctuations are of a similar magnitude (approximately 10 cm per day) as the inline fluctuations. These large diurnal flow-field variations have never before been observed because they average to zero over the course of the longer-period observations such as repeat interferometric SAR or repeat multi-day GPS solutions. We speculate that the crossline flow is from the tilt of the ice shelf caused by the tide phase difference between the north and south ends of the ice shelf [*Padman et al.*, 2002], but more research is needed. Understanding the mechanism for induc-

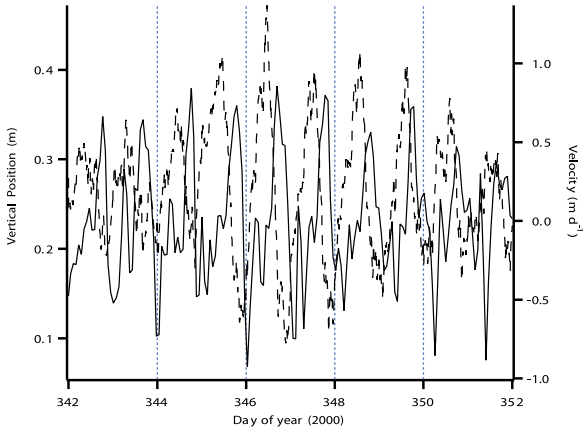

Figure 3. Velocity fluctuations at the grounding line with the mean removed (site K0) plotted with a solid line (scale on the right axis) and the vertical displacement (tidal signal) plotted with a dashed line and with scale along the left axis.

ing large-amplitude lateral flow, at high frequency, transmitted well inland is a challenge in ice-stream flow research.

2.2. Flow Field Upstream of the Grounding Line

[10] The flow speed variations at K40 are similar to those at K0, as shown by the cross-correlation of the position data (Figure 5) as well as a qualitative examination of the plots in Figure 2. The cross-correlation of the inline positions shows a strong peak at a lag of 1.1 ± 2 hrs. The peak is a relatively broad one, with correlations of greater than 90% of the peak value within ±2 hrs of the peak. We correlate position data because the velocity data are noisier as they are the derivative of the position; we are only interpreting the time lag, which is unchanged by differentiation, and not the amplitude, which scales by frequency. The flow at K80 also shows flow fluctuations similar to K0 but with a lag of 3.1 ± 2 hrs.

3. Interpretation and Discussion

[11] Here we follow the model of *Anandakrishnan and Alley*, [1997] (hereinafter referred to as AA97), in which the

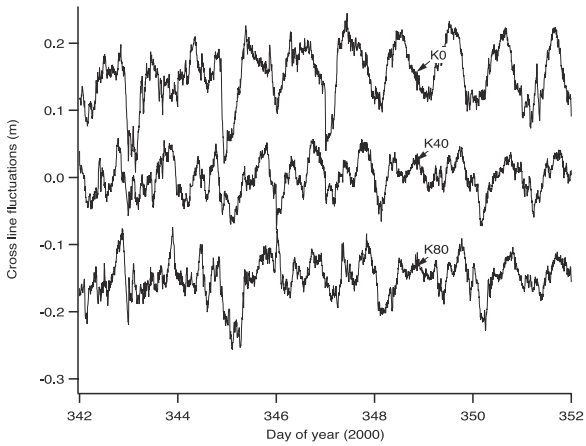

Figure 4. Crossline flow fluctuations at the three ice stream sites: K0, upper curve, K40, middle curve, and K80, lower curve. As in Figure 2 the curves all have had their mean subtracted, and then K0 and K80 have been offset for display purposes.

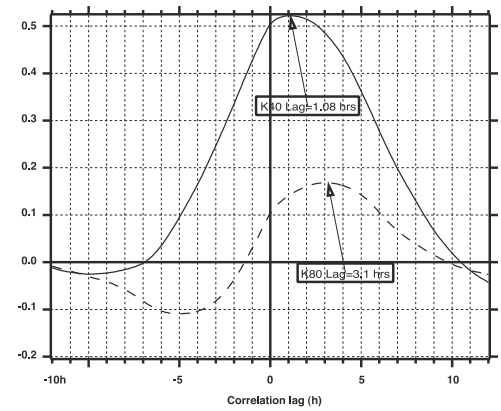

Figure 5. Cross correlation of the flow fluctuations at K0 and K40 (solid curve) and the fluctuations at K0 and K80 (dashed curve).

forcing at the grounding line travels up the ice stream at a velocity of propagation (phase velocity ν) that depends on the viscosity of the ice stream substrate coupled to the overlying ice, which is nearly elastic at these frequencies. The flow fluctuations at K0 are the response to the tide at the grounding line, and the flow fluctuations at K40 and K80 are the responses to a travelling stress wave. Local earth tides [*Kulessa et al.*, 2003; *Bredehoeft*, 1967] are unlikely to be the cause of the velocity fluctuations for two reasons: (1) the magnitude of the displacement fluctuation decays with distance from the grounding line, and (2) there is measurable delay in this signal at K80 and at K40 relative to K0. As earth tides do not have a large phase difference over the 80 km of our experiment, it is unlikely that the response to the forcing would have different delays at different locations.

[12] The ice stream response to the tidal forcing is delayed by 1.1 ± 2 hrs at K40, and 3.1 ± 2 at K80, relative to the response at K0. By using the difference in lags between K40 and K80, and the known distance between them, we obtain ν = 40 km/2hrs = 5.6 m · s^{-1} (the distance between K40 and K80 divided by the difference in lags). While the uncertainties of the estimate encompass a broad range of velocities of propagation, the likely velocity is on the order of meters per second. This velocity is much less than the $O(10^3$ m · s$^{-1})$ of an elastic wave on the ice stream, and is interpretable as the delaying effect of time-dependent deformation of the substrate (deforming till; *Kamb* [2001]) to which the ice stream is coupled.

[13] We calculate the properties of the ice stream D substrate using Eq. 21 of AA97, in which the "basal stiffness" $S = \eta/h_b$ can be determined from the phase velocity ν. The basal stiffness is the ratio of the viscosity of the basal layer η to its thickness h_b. We determine $S = 1.5 \times 10^7$ Pa s m^{-1}. Thus we suggest that the substrate beneath ice stream D is an order-of-magnitude weaker than the basal layer for the neighboring slow-flowing ice stream C ($S = 1.5 \times 10^8$ Pa s m^{-1}). *In situ* borehole observations also indicate somewhat stiffer till under ice stream C than under ice stream D, although differences in the loading configuration prevent detailed quantitative comparison [*Alley*, 2000; *Kamb*, 2001]. The "penetration distance" X is the distance at which the forcing at the grounding has decayed to $1/e$ of its initial amplitude. From Eq. 22 of AA97, $X \propto S^{-1/2}$,

implying that the travelling wave will penetrate farther upstream on ice stream D than did the disturbance on ice stream C, a testable hypothesis with additional GPS data.

[14] The relatively small stresses (O(0.1 bar)) and short times (diurnal) associated with tidal loading of the end of the ice stream allow an elastic model for the primarily cold ice along the ice-stream midline (AA97). However, in the ice-stream shear margins where high mean stresses and deformational heating favor faster deformation, which probably increases as the cube of the shear stress [*Raymond et al.*, 2001], creep relaxation of elastic strains may be important. Oscillating stresses together with the cubic dependence of strain rate on stress will cause the mean shear stress needed to allow the observed mean ice-stream velocity to be smaller than in the absence of tidal forcing. Our data are from the ice plain, where side shear stresses are relatively less important, and from the transition to the main ice stream with more-important side shear. Additional data from farther upglacier, combined with careful analysis, will be required to assess the impact of tidal effects on the side shear stress, and thus on the force balance and calculated basal shear stress of the ice stream, but it is likely that there is some effect.

[15] The nonsteadiness associated with the tidal forcing also may affect properties of the ice-stream basal till. *Moore and Iverson* [2001] (also see *Iverson et al.* [1998] and *Alley* [2000]) showed that shear loading of remolded, overconsolidated till samples led to deformation and dilation, causing pore-water pressure to drop, which strengthened the sediment until sufficient water inflow occurred; ultimate failure was delayed until critical-state porosity was reached. Although subglacial conditions are not exactly analogous, varying basal stress from tidal forcing may force water exchange between subglacial till and the ice-contact water-drainage system, and prevent steady-state conditions in the till. The additional strength likely imparted to the basal sediments by the nonsteadiness associated with the tidal signal may serve to balance the larger basal shear stress likely associated with the tidal softening of the shear margins. This may contribute to the apparently viscous behavior of the ice-stream bed, which shows clear time-delay compared to elastic propagation of the tidal signal despite the expectation from experiments taken to steady deformation that behavior would be perfectly plastic [*Kamb*, 2001].

[16] Pending additional data and analyses, it is clear that tidal forcing greatly affects the flow of large West Antarctic ice streams (AA97; *Bindschadler et al.* [2003]; this work), in poorly understood but probably important ways. Analyses of multi-day ice stream flow measurements need to account for this phenomenon in their interpretations.

[17] **Acknowledgments.** We thank J Bowling, JE Voigt, Kenn Borek Air and pilots, and the University NAVSTAR Consortium (UNAVCO) staff for assistance with the field work. We thank P. Vornberger and I. Joughin for generous contributions of time and data. This work was supported by the National Science Foundation (NSF-OPP 9996272).

References

Alley, R. B., Continuity comes first: Recent progress in understanding subglacial deformation, in *Deformation of Glacial Materials*, edited by A. J. Maltman and M. J. Hambrey, *Geol. Soc. Spec. Publ.*, *176*, 171–179, 2000.

Anandakrishnan, S., and R. B. Alley, Tidal forcing of basal seismicity of ice stream C, West Antarctica, observed far inland, *J. Geophys. Res.*, *102*, 15,183–15,196, 1997.

Bindschadler, R., P. L. Vornberger, M. King, and L. Padman, Diurnal stick-slip motion in the mouth of Whillans Ice Stream, *Ann. Glaciol*, in press, 2003.

Bredehoeft, J. D., Response of well-aquifer systems to Earth tides, *J. Geophys. Res.*, *72*, 3075–3087, 1967.

Doake, C. S. M., R. M. Frolich, D. R. Mantripp, A. M. Smith, and D. G. Vaughan, Glaciological studies on Rutford Ice Stream, Antarctica, *J. Geophys. Res.*, *92*, 8951–8960, 1987.

Doake, C. S. M., H. F. J. Corr, K. W. Nicholls, A. Gaffikin, A. Jenkins, W. I. Bertiger, and M. A. King, Tide-induced lateral movement of Brunt Ice Shelf, Antarctica, *Geophys. Res. Lett.*, *29*(8), 1226, 10.1029/2001GL014606, 2002.

Engelhardt, H., and W. B. Kamb, Basal sliding of ice stream B, West Antarctica, *J. Glaciol.*, *44*, 223–230, 1998.

Goldstein, R. M., H. Engelhardt, W. B. Kamb, and R. M. Frohlich, Satellite radar interferometry for monitoring ice sheet motion: Application to an Antarctic ice stream, *Science*, *262*, 1525–1530, 1993.

Harrison, W. D., K. A. Echelmeyer, and H. Engelhardt, Short-period observations of speed, strain and seismicity on ice stream B, Antarctica, *J. Glaciol.*, *39*, 463–470, 1993.

Iverson, N. R., T. S. Hooyer, and R. W. Baker, Ring-shear studies of till deformation: Coulomb-plastic behavior and distributed strain in glacier beds, *J. Glaciol.*, *44*, 634–642, 1998.

Joughin, I., L. Gray, R. Bindschadler, S. Price, D. Morse, C. Hulbe, K. Mattar, and C. Werner, Tributaries of West Antarctic ice streams revealed by RADARSAT interferometry, *Science*, *286*, 283–286, 1999.

Kamb, B., Basal zone of the West Antarctic ice streams and its role in the lubrication of their rapid motion, in *TheWest Antarctic Ice Sheet: Behavior and Environment*, *Antarct. Res. Ser.*, vol. 77, edited by R. B. Alley and R. A. Bindschadler, pp. 157–200, AGU, Washington, D. C., 2001.

King, M. A., and S. Aoki, Tidal observations on floating ice using a single GPS receiver, *Geophys. Res. Lett*, doi:10.1029/2002GL016182, in press, 2003.

Kulessa, B., B. P. Hubbard, G. H. Brown, and J. Becker, Earth tide forcing of glacier drainage, *Geophys. Res. Lett*, doi:10.1029/2002GL015303, in press, 2003.

Lichten, S. M., Estimation and filtering for high-precision GPS positioning applications, *Manuscr. Geod.*, *15*, 159–176, 1990.

Liu, H., K. Jezek, B. Li, and Z. Zhao, Radarsat Antarctic mapping project digital elevation model version 2, http://nsidc.org/data/nsidc-0082.html, Natl. Snow and Ice Data Cent., Boulder, Colo., 2001.

MacAyeal, D. R., Numerical simulations of the Ross Sea tides, *J. Geophys. Res.*, *89*, 607–615, 1984.

Moore, P. L., and N. R. Iverson, Stick-slip deformation of sediment due to cyclic dilatant hardening, *Eos Trans. AGU*, *82*(47), Fall Meet. Suppl., S51C-06, 2001.

Padman, L., H. A. Fricker, R. Coleman, S. Howard, and S. Erofeeva, A new tidal model for the Antarctic ice shelves and seas, *Ann. Glaciol.*, *34*, 247–254, 2002.

Raymond, C. F., K. A. Echelmeyer, I. M. Whillans, and C. S. M. Doake, Ice stream shear margins, in *The West Antarctic Ice Sheet: Behavior and Environment*, *Antarct. Res. Ser.*, vol. 77, edited by R. B. Alley and R. A. Bindschadler, pp. 137–155, AGU, Washington, D. C., 2001.

Smith, A. M., The use of tiltmeters to study the dynamics of Antarctic ice-shelf grounding lines, *J. Glaciol.*, *37*, 51–58, 1991.

Williams, R. T., and E. S. Robinson, The ocean tide in the southern Ross Sea, *J. Geophys. Res.*, *85*, 6689–6696, 1980.

Zumberge, J. F., M. B. Heflin, D. C. Jefferson, M. M. Watkins, and F. H. Webb, Precise point positioning for the efficient and robust analysis of GPS data from large networks, *J. Geophys. Res.*, *102*, 5005–5017, 1997.

R. B. Alley, S. Anandakrishnan, and D. E. Voigt, Earth and Mineral Sciences Environment Institute, Department of Geosciences, Pennsylvania State University, 204A Deike Building, University Park, PA 16802, USA. (ralley@essc.psu.edu; sak@essc.psu.edu)

M. A. King, School of Civil Engineering and Geosciences, University of Newcastle Upon Tyne, Newcastle Upon Tyne NE1 7RU, U. K. (m.a.king@ncl.ac.uk)